



Mechanics of the Interface Interaction between Hemp Fibers and Compacted Clay

Ashtarout Ammar, M.E.¹; Shadi Najjar, Ph.D., A.M.ASCE²; and Salah Sadek, Ph.D., M.ASCE³

Abstract: A drive is currently underway in the construction industry to promote the use of *in situ* soils (including clays) that are reinforced with natural fibers. This effort is primarily driven by sustainability considerations and concerns. Understanding of the interface resistance between natural fibers and clays is critical for reliably predicting the response of structures that are built on, or with, fiber-reinforced clays. The objective of this paper was to investigate the interface shear strength between natural hemp fibers and clay through interface direct shear and single fiber pullout tests. The parameters that were varied are the compaction water content and the drainage condition at the interface. The results indicated that the interface shear strength parameters are significantly affected by the test mechanism and drainage conditions. For compacted fiber-reinforced clay systems that are governed by short-term stability conditions, interface interaction coefficients may be best quantified using fast single fiber pullout tests. For systems that are governed by long-term stability, the drained interface friction coefficient could be estimated using small-scale direct shear or single fiber pullout tests. Hemp fibers are relatively efficient at mobilizing the shear strength of the clay, with interface interaction coefficients that could approach unity. DOI: [10.1061/\(ASCE\)GM.1943-5622.0001368](https://doi.org/10.1061/(ASCE)GM.1943-5622.0001368). © 2019 American Society of Civil Engineers.

Author keywords: Compacted soils; Fiber-reinforced clay; Soil–fiber interface; Shear strength; Pullout resistance; Discrete fibers.

Introduction and Background

The reinforcement of soils using inclusions has gained wide interest in a number of geotechnical applications. The aim of soil reinforcement is to improve the stability of geotechnical systems and reduce vertical and lateral deformations. Traditionally, geosynthetics, geotextiles, geofibers, and geogrids have been widely used as inclusions in geotechnical engineering systems (Hossain et al. 2012). Over the past two decades, there has been interest in utilizing randomly distributed fibers as reinforcement inclusions to enhance the engineering characteristics of various soil types owing to advantages associated with the “absence” of potential planes of weakness (Maher and Gray 1990), added ductility and strength (Ola 1989), and reduction in shrink/swell potential (Soltani et al. 2018). Hejazi et al. (2012) reported that several geotechnical engineering applications that involve pavements, retaining walls, railway embankments, protection of slopes, seismic mitigation, and foundation support have used discrete fibers in their implementation.

Due to sustainability considerations, there is a current drive in the construction industry that advocates the use of eco-composite

materials that are environmentally friendly and can provide viable substitutes for synthetic materials. In fact, natural fibers have long been used in many developing countries in cement composites and earth blocks given their availability and low cost (Hejazi et al. 2012). Several studies (Prabakar and Sridhar 2002; Bouhicha et al. 2005; Li et al. 2006; Lin et al. 2010; Dittenber and GangaRao 2012; Najjar et al. 2014; Wang et al. 2017, 2018; Lu et al. 2017) have investigated the potential use of natural fibers and other sustainable materials in reinforcing sandy and clayey soils. The results indicated that soils that are reinforced with natural fibers generally exhibit improved strength and ductility.

Hemp fibers are natural fibers that originate from the plant *Cannabis sativa*. Hemp is legally planted in different countries and is used in several industries such as paper, textiles, clothing, biodegradable plastics, construction, cosmetic products, health foods, and biofuel. Hemp grows from a seed to maturity in approximately 12–16 weeks. It is considered one of the most important types of natural fibers for industrial applications. According to Wang (2002), hemp has a high tensile strength and strong tolerance for an alkali environment, which makes it a good reinforcement material. Najjar et al. (2014) and Abou Diab et al. (2016, 2018) investigated the improvement that is brought by the addition of hemp fibers to the undrained strength of compacted clays. They concluded that hemp is effective in increasing the undrained shear strength and ductility of the reinforced clay.

The properties of the soil–fiber interface play an important role in dictating the response of the fiber-reinforced soil, regardless of the type of fiber. Although considerable research has been devoted to the investigation of the shear strength of the “fiber-reinforced soil” as a matrix, less attention has been given to characterize the interface parameters between the soil and the fiber. Some studies have investigated the soil–interface behavior between solids and sands (Bosscher and Ortiz 1987; Kishida and Uesugi 1987; Jewell and Wroth 1987; Paikowsky et al. 1995; Hossain et al. 2012; Bacas et al. 2015; Cardile et al. 2016; Punetha et al. 2017) and between solids and clays (Ellithy and Gabr 2000; Lemos and Vaughan 2000;

¹Research Assistant, Dept. of Civil and Environmental Engineering, American Univ. of Beirut, P.O. Box 11-0236, Riad El-Solh, Beirut 1107-2020, Lebanon. Email: ashtarout.ammar@hotmail.com

²Associate Professor, Dept. of Civil and Environmental Engineering, American Univ. of Beirut, P.O. Box 11-0236, Riad El-Solh, Beirut 1107-2020, Lebanon (corresponding author). ORCID: <https://orcid.org/0000-0003-1824-4540>. Email: sn06@aub.edu.lb

³Professor, Dept. of Civil and Environmental Engineering, American Univ. of Beirut, P.O. Box 11-0236, Riad El-Solh, Beirut 1107-2020, Lebanon. Email: salah@aub.edu.lb

Note. This manuscript was submitted on March 30, 2018; approved on September 11, 2018; published online on February 1, 2019. Discussion period open until July 1, 2019; separate discussions must be submitted for individual papers. This paper is part of the *International Journal of Geomechanics*, © ASCE, ISSN 1532-3641.

Zornberg 2002; Miller and Hamid 2007; Khoury et al. 2011; Jamie et al. 2013; Hatami and Esmaili 2015; Ferreira et al. 2015; Tang et al. 2016). In these studies, either direct shear tests or pullout tests were conducted to study the interaction between the soil and the reinforcement. Results from these tests indicate that the compaction water content of the soil plays a significant role in determining the interface properties. Moreover, the interface strength was observed to be significantly affected by the rate of loading and drainage conditions.

A closer investigation of the scope and findings of previous work on solid–clay interfaces shows that the focus has been on the interface behavior between clays and geosynthetics or geogrids, rather than on randomly distributed fibers. These studies have emphasized the drained response and less attention has been paid to the undrained behavior, which may govern short-term stability problems in the field. More importantly, previous research is lacking in reference to specific studies addressing natural fibers and their interface characteristics when used as inclusions in clayey soils. The objective of the present study was to investigate the interface response between natural clay and hemp fibers with a focus on three main parameters: the compaction water content, the type of interface test, and the drainage conditions and rate of loading. This study supplements the literature with much needed, high quality, interface strength data that results from two well-known interface testing methodologies (direct shear and single fiber pullout).

Material Properties and Experimental Setup

Materials

The soil used in the present study was of natural origin. Its properties are summarized in Table 1. The soil was classified as “inorganic clay of low plasticity” (CL) in the unified soil classification system (USCS). The clay had a plasticity index (PI) of 14% and a fines content of around 55%. The clay fraction within the fines was around 35%. Results from X-ray diffraction tests on the clay fraction indicated a predominance of kaolinite minerals. Although the soil was classified as a clay, it contained a significant percentage of sand.

Standard Proctor compaction tests were conducted to determine the maximum dry unit weight and optimum moisture content, which were found to be 16.8 kN/m^3 and 19%, respectively. It should be noted that the soil used in the present study is typical of natural non-ideal soil materials that are abundant in many geological settings but not thoroughly studied in typical research contexts.

The natural fibers used in the present study were hemp fibers. They were imported as long fibers in the form of a fiber bundle (Fig. 1). Fibers were treated to eliminate organic impurities via soaking in a sodium hydroxide (NaOH) solution at 6% by weight for 48 h. After treatment, they were thoroughly washed with clean water and left to air dry. The properties of the fibers are presented in Table 2.

The fibers had a rectangular cross section with a wide variability in dimensions. The thickness of the fibers was relatively uniform with an average of 0.13 mm, whereas the width was relatively variable with an average of 0.65 mm and a standard deviation of 0.42 mm. The average ultimate tensile strength was determined to be 276 MPa, with a range varying from 181 to 415 MPa. The modulus of elasticity ranged from 16.1 to 29.8 GPa, with an average of 21.7 GPa. A microphotograph showing a single hemp fiber and a sample of soil under scanning electron microscopy (SEM) is presented in Fig. 2. The microstructure of hemp consists of cellulose

Table 1. Material properties of the soil

Property	Value
Specific gravity	2.65
Liquid limit [LL (%)]	34
Plasticity index [PI (%)]	14
D_{50} (mm)	0.035
Sand (%)	46
Silt (%)	32
Clay (%)	22
Optimum water content (%)	19
Maximum dry unit weight (kN/m^3)	16.8
Predominant mineral in coarse fraction	Quartz
Predominant mineral in clay fraction	Kaolinite



Fig. 1. Bundle of hemp fibers and typical compacted soil specimen. (Images by Shadi Najjar.)

Table 2. Material properties of the hemp fibers

Fiber property	Value
Specific gravity	1.4
Ultimate tensile strength [mean (MPa)]	276
Elastic Modulus [mean (GPa)]	21.7
Thickness [mean (mm)]	0.13
Width [mean (mm)]	0.65
Major constituent	Cellulose
Roughness [air dry (μm)]	2.1
Roughness [wet (μm)]	1.8
Water content {air dry [mean (%)]}	8
Absorption capacity [mean (%)]	90

microfibrils that are embedded in a matrix of hemicelluloses and/or lignin. Additional details pertaining to the microstructure of hemp can be found in Fan (2010). Water content and water absorption tests indicate that hemp fibers have an average air-dried water content of about 8% and an average water-absorption capacity of about 90%.

The fiber roughness was measured using a highly sensitive profilometer. Roughness was measured along the fiber surface in the longitudinal section under dry and wet conditions. Multiple sets of measurements were collected along the fiber surface. The average roughness was found to be equal to $2.10 \mu\text{m}$ in the case of air-dried fibers and $1.8 \mu\text{m}$ in the case of wet fibers. The surface roughness values were generally larger than typical roughness values for geomembranes and geogrids.

Experimental Program

The interface shear resistance between the clay and fibers was measured using a series of interface direct shear tests and single fiber pullout tests. The compaction water content, the applied normal stress, and the rate of shearing/pullout (rapid/“undrained” versus slow/drained) were varied in the experimental program. The clay specimens were compacted at different water contents to simulate dry of optimum ($w = 14\%$) and around optimum (18% and 20%) conditions. In the rapid/undrained tests, the specimens were tested as-compacted. In the slow/drained tests, the specimens were given access to water and allowed to consolidate under the applied normal stress.

In a first series of tests, 36 clay–clay and clay–hemp interface direct shear tests were performed on compacted natural clay that was prepared by kneading using the miniature Harvard compactor (Wilson 1970). In the second series of tests, 18 single fiber pullout tests were conducted, where a single fiber was sandwiched between two layers of compacted clay prepared using the same method. The dry soil was initially mixed with water, placed in a split mold in

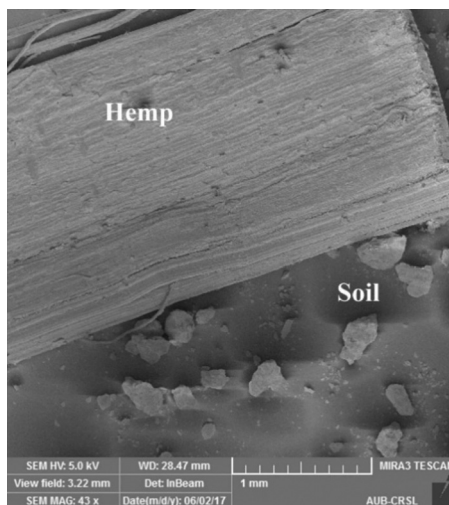


Fig. 2. Scanning electron microscopy image of a single hemp fiber and some soil (43 \times magnification). (Image by Shadi Najjar.)

batches of equal thicknesses, and compacted using the Harvard apparatus. The apparatus consists of a small-diameter cylindrical rod that is used to apply a controllable pressure onto the soil. In direct shear tests, the specimens were compacted in a split mold with a height of 21 cm and a diameter of 7.15 cm. For the pullout tests, cylindrical specimens with a height of 20 cm and a diameter of 8.25 cm were prepared.

The kneading effort that was required to compact the specimens involved two steps. In the first step, the standard Proctor compaction curve of the soil was established using five specimens that were compacted at different water contents. In the second step, the dry unit weight of the soil specimens compacted by the kneading pneumatic compactor was assessed under different combinations of number of layers, number of tamps per layer, and tamping pressure. The required kneading effort consisted of five layers for the direct shear test specimens and six layers for the pullout test specimens with each layer compacted by 25 tamps at a tamping rod pressure of 10 psi. The objective was to reach target dry unit weights of about 95–100% of the standard Proctor dry unit weight as recommended by common construction specifications. The need for different compaction efforts between direct shear and pullout specimens is related to differences in the dimensions of the specimens. Following the compaction process, the specimen was extracted from the split mold, trimmed to the required height (Fig. 1), and assembled in the respective testing apparatus. Fig. 3 gives the as-compacted properties (initial water content and dry density) of the direct shear [Fig. 3(a)] and pullout [Fig. 3(b)] specimens in comparison to the Standard Proctor compaction curve. It should be noted that the data points in Fig. 3 are limited to those used to conduct as-compacted quick undrained tests.

The first series of direct shear tests consisted of conventional clay–clay tests. The second series consisted of direct shear interface tests in which the clay specimen was fixed in the upper part of the shear box and sheared against individual hemp fibers (width of about 2–3 mm) that were glued onto a steel plate in the lower part of the shear box (Fig. 4). The fibers were glued in an orientation that is in line with the relative displacement between the two boxes. A circular shear box with an internal diameter of 63.5 mm and a height of 50.8 mm was used. The thickness of the test specimens was about 20 mm in the clay–clay tests and 10 mm in the clay–hemp interface tests. This maintained the actual soil thickness that was being sheared at 10 mm in both types of tests (one-half of the specimen in

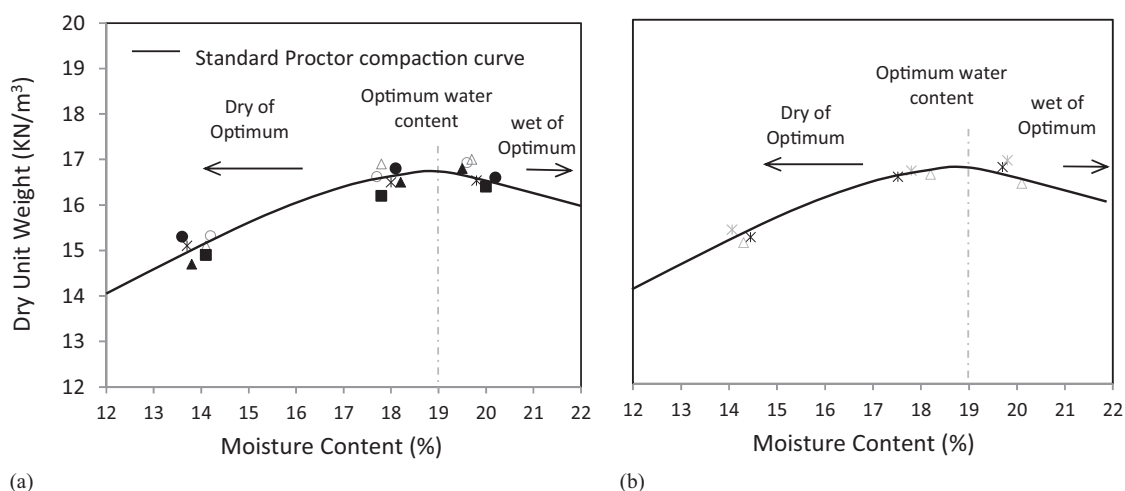


Fig. 3. Compaction characteristics of soil specimens compared with Standard Proctor compaction curve (data points for undrained tests only): (a) direct shear; and (b) pullout tests.

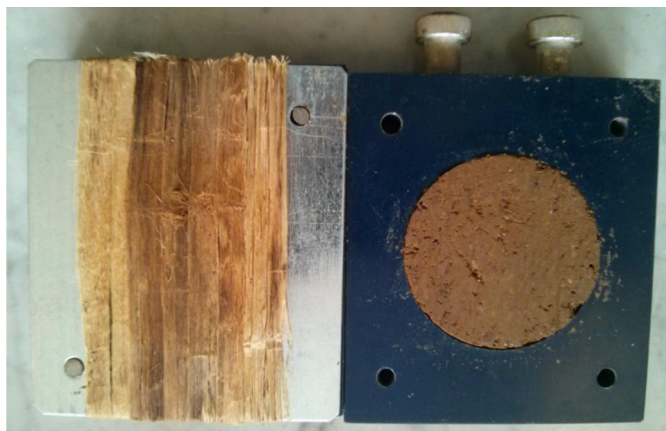


Fig. 4. Direct shear mold with clay in the upper half and hemp glued to a steel plate on the lower half. (Images by Shadi Najjar.)

clay–clay tests and the full specimen in the interface tests). A gap of about 0.6–0.7 mm (~ 15 times D_{50}) was maintained between the two parts of the shear box during shear, where D_{50} is defined as the grain size with 50% of the soil smaller than that size.

Two types of direct shear tests were conducted in the present study. The aim was to understand the interface behavior between hemp fibers and clay under two extreme conditions. The first condition targeted the short-term response of “as-compacted” unsaturated specimens that were not allowed to consolidate under the normal stress, were sheared in a fast shearing rate (1.3 mm/min) to minimize drainage during shearing, and were not allowed access to water during consolidation and shearing. The second condition targeted the long-term response where the compacted specimens were allowed to consolidate for 24 h, sheared at a slow shear rate of 0.025 mm/min, and allowed access to water throughout consolidation and shearing. The “quick” tests were modeled to represent unconsolidated–“undrained” loading conditions with minimal dissipation of pore water pressures during shear, whereas the “slow” tests represent typical consolidated drained behavior.

Given the lack of control of drainage in a direct shear setup, it is difficult to ensure a fully undrained response, even upon the selection of a fast shear rate. However, it is expected that at a rate of shear of 1.3 mm/min, the fast tests could be considered to be representative of relatively undrained conditions. Fleming et al. (2006) stated that rates higher than 0.83 mm/min are generally used to simulate undrained conditions in direct shear tests. Ellithy and Gabr (2000) used a rate of 2 mm/min to simulate undrained conditions in interface tests between kaolinite clay and two geomembranes. Abu-Farsakh et al. (2007) used a rate of 0.85 mm/min to conduct undrained tests between three clays and a number of geogrid and geotextile interfaces. Two of the clays had relatively low PIs of 6 and 25 (compared with $PI = 14$ in our study). The compaction curves of these clays were very similar to that of the clay used in our study.

The choice of the slow shearing rate of 0.025 mm/min in the “drained” tests was guided by the rates used in similar published studies, taking into account the difference in soil composition and plasticity, and confirmed by the time-rate of consolidation witnessed in the normal stress application phase. With regard to the published literature, Koerner et al. (1986) used a shear rate of 0.06 mm/min to measure the drained clay–clay and clay–interface strength between five geomembranes and five compacted unsaturated cohesive soils with PI values ranging from 8 to 72. Gan et al. (1988) reported that the drained peak shear

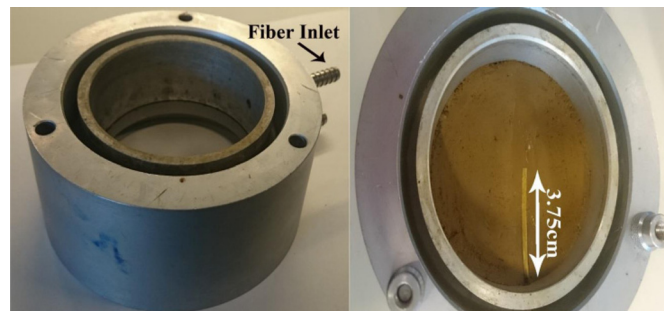


Fig. 5. Pullout test setup with hemp fiber sandwiched between compacted clay. (Images by Shadi Najjar.)

stress of a clay ($PI = 18.7$) was unaffected up to a shear rate of 0.013 mm/min. Mirzababaei et al. (2017, 2018a) also used a horizontal displacement rate of 0.01 mm/min to maintain drained condition during drained direct shear tests. The shearing rate of 0.025 mm/min used to simulate drained loading in our study was smaller than that used by Koerner et al. (1986). The drained conditions could also be confirmed by the relatively small t_{50} (ranging from 0.5 to 5 min) values that were witnessed in the consolidation phase of the clay–interface and clay–clay tests. Although the specimens were not fully saturated during consolidation, these values of t_{50} are indicative of the permeability of the soil. The rate of 0.025 mm/min ensured that the time to failure was within $50t_{50}$.

Pullout tests were conducted using a modified one-dimensional consolidation ring that was customized to allow for the insertion of a single fiber between two layers of compacted clay (Fig. 5). A 1-cm thick clay specimen was first placed within the ring. The fiber was then inserted horizontally within the fabricated hole and allowed to rest on top of the clay, with an embedment length of 3.75 cm. A second 0.5-cm thick clay specimen was then placed on top, sandwiching the fiber between the two specimens. Following the placement of the consolidation ring cap and application of the normal load, the fiber was then pulled out horizontally using a thin cable and pulley system. The load was provided/controlled by attaching a water container to the cable and filling it as desired (Fig. 6). The rate at which water was added to the container was controlled using a sensitive burette. In the “slow” tests, samples were consolidated under the normal stress and the fiber was pulled out slowly. The load was applied in increments with a 30-min period separating two consecutive increments to ensure dissipation of pore water pressure. For the “quick” tests, samples were not allowed to consolidate and the fiber was pulled at a fast rate through a continuous flow of water into the container, with pullout generally occurring within 1–3 min.

Results

Direct Shear Tests

Shear Stress versus Horizontal Displacement Relationship

The variation of the shear stress with horizontal displacement for clay–clay and clay–hemp tests is presented in Figs. 7(a, c, and e) and 7(b, d, and f) for the as-compacted “quick” tests and the consolidated drained tests, respectively. For all clay–clay tests, the applied shear stress was calculated by dividing the measured horizontal force by the corrected area A_c , which was calculated for the case of a circular direct shear box as indicated in Eq. (1)

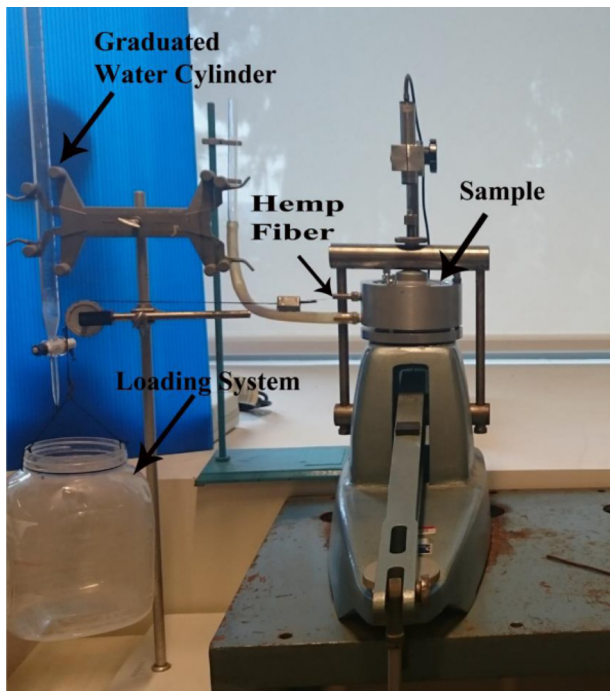


Fig. 6. Setup of the single fiber pullout test. (Image by Shadi Najjar.)

$$A_c = r^2 (2\alpha - \sin 2\alpha) \quad (1)$$

where $\alpha = \cos^{-1}(\Delta x/2r)$ is in radians and r and Δx are the radius of the test specimen and the applied horizontal displacement, respectively. It should be noted that no area corrections were required in the analysis of the interface direct shear tests because the base plate was designed to ensure continuous hemp–soil contact during shearing.

Results from the as-compacted quick/undrained tests [Figs. 7(a, c, and e)] on the clay–clay specimens indicate a relatively high sensitivity of the shear stress versus displacement response to the initial water content and the applied total normal stress. No peaks were observed in the shear stress versus horizontal displacement response except for tests conducted at $\sigma_n = 20$ kPa. The brittle, softening response at 20 kPa was pronounced at lower compaction water contents where the soil exhibited lower degrees of saturation ($S \sim 45\text{--}55\%$ for $w = 14\%$ and $75\text{--}85\%$ for $w = 18\%$) and a more flocculated internal structure. The softening response could be attributed to the possible tendency of expansive volume change for unsaturated compacted soil against the relatively low normal stresses and to the reorientation in the internal structure/fabric of the clay during the shearing process. The tendency for expansive volume change was expected given the composition of the soil, which contained more than 45% sand in its matrix. More importantly, results in Figs. 7(a, c, and e) indicate that at any given normal stress, specimens that were compacted at lower water contents were able to carry higher shear stresses at failure. This is possibly related to the higher initial matric suction that is expected to exist at lower degrees of saturation.

In the consolidated drained clay–clay tests where the clay was allowed to exchange water freely with the water bath during all stages [Figs. 7(b, d, and f)], the shear stress versus displacement curves indicated a strain hardening response that was sensitive to the normal/consolidation stress and relatively insensitive to the initial compaction water content. At any given consolidation stress, the relative insensitivity of the response to the initial compaction

water content is attributed to a “saturation” process that could have increased the as-compacted water content and reduced the impact of the initial matric suction, rendering the response more sensitive to the applied consolidation stress, dry density after consolidation (prior to shear), and the soil structure and composition.

On the other hand, results pertaining to the clay–hemp tests (Fig. 7) indicate a strain softening response with clear peaks in the interface shear stress at relatively small displacements (0.5–1.5 mm). Interestingly, fast interface tests with as-compacted specimens and drained interface tests with specimens that were consolidated prior to shear showed more-or-less similar responses for any given water content and applied normal stress. Unlike the fast clay–clay tests where the results of the as-compacted specimens showed a strong dependency on the initial water content, the response in the fast clay–hemp interface tests was very similar to that of the drained interface tests, pointing to possible drainage or disruption of menisci at the interface, even under fast loading conditions. This issue will be further investigated in the following section.

Effect of Water Content on the Clay–Clay and Clay–Hemp Shear Strength

The maximum shear stresses observed for all direct shear tests (clay–clay and clay–hemp) are presented in Fig. 8 as a function of the compaction water content for both undrained [Figs. 8(a and c)] and drained [Figs. 8(b and d)] loading conditions, respectively.

An investigation of the maximum shear stresses mobilized in the quick clay–clay tests on as-compacted specimens indicated a clear reduction in the maximum shear stress with an increase in the compaction water content. The percentage decrease in the maximum shear stress for specimens compacted at $w = 18\%$ and 20% relative to the driest specimen ($w = 14\%$) was calculated for all normal stresses and plotted in Fig. 9. The results indicate that the maximum clay–clay shear stresses decrease by about 28.1–34.8% (depending on the applied normal stress) when the as-compacted water content increases from 14% (saturation $\sim 50\%$) to 18% (saturation $\sim 80\%$). An increase in the water content to 20% (saturation $\sim 90\%$) decreases the maximum shear stress by about 31.1% ($\sigma_n = 20$ kPa) to 41.6% ($\sigma_n = 200$ kPa) compared with the $w = 14\%$ sample.

The observed decrease in the as-compacted undrained shear strength of clays with increasing water content is in line with published results. Ellithy and Gabr (2000) report a drop of 77% in the undrained shear stress of kaolinite clay when the water content was increased from 28% (2% dry of optimum) to 32% (2% wet of optimum). Similar results were reported by Abu-Farsakh et al. (2007) who observed average shear stress decreases of approximately 20% and 31% as the water content of an CL-ML soil (PI = 6) was increased from 12% (dry of optimum) to 18.8% (optimum) and 21.0% (wet of optimum), respectively. Decreases of approximately 16 and 35% were also observed for a CL clay (PI = 25) as the water content was increased from 11 to 16.5% (optimum) and 20%, respectively. The reduction in the as-compacted unsaturated shear strength of clays with water content is generally attributed to a reduction in the matric suction at larger water content; changes to the flocculated clay fabric/structure, which tends to be more oriented/dispersed at larger water contents; and possible development of positive pore water pressure during fast shearing as the clay approaches saturation at higher water contents (Seed and Boulanger 1991; Ellithy and Gabr 2000; Fleming et al. 2006; Abu-Farsakh et al. 2007; Hatami and Esmaili 2015).

It is worth noting that the specimens compacted around the optimum water content of 18 and 20% had almost the same dry density of approximately 16.5 kN/m³ (Fig. 3), whereas the specimen compacted dry of optimum at $w = 14\%$ had a lower dry density (~ 15.0 kN/m³). Results in Fig. 8(a) indicate that the specimen at

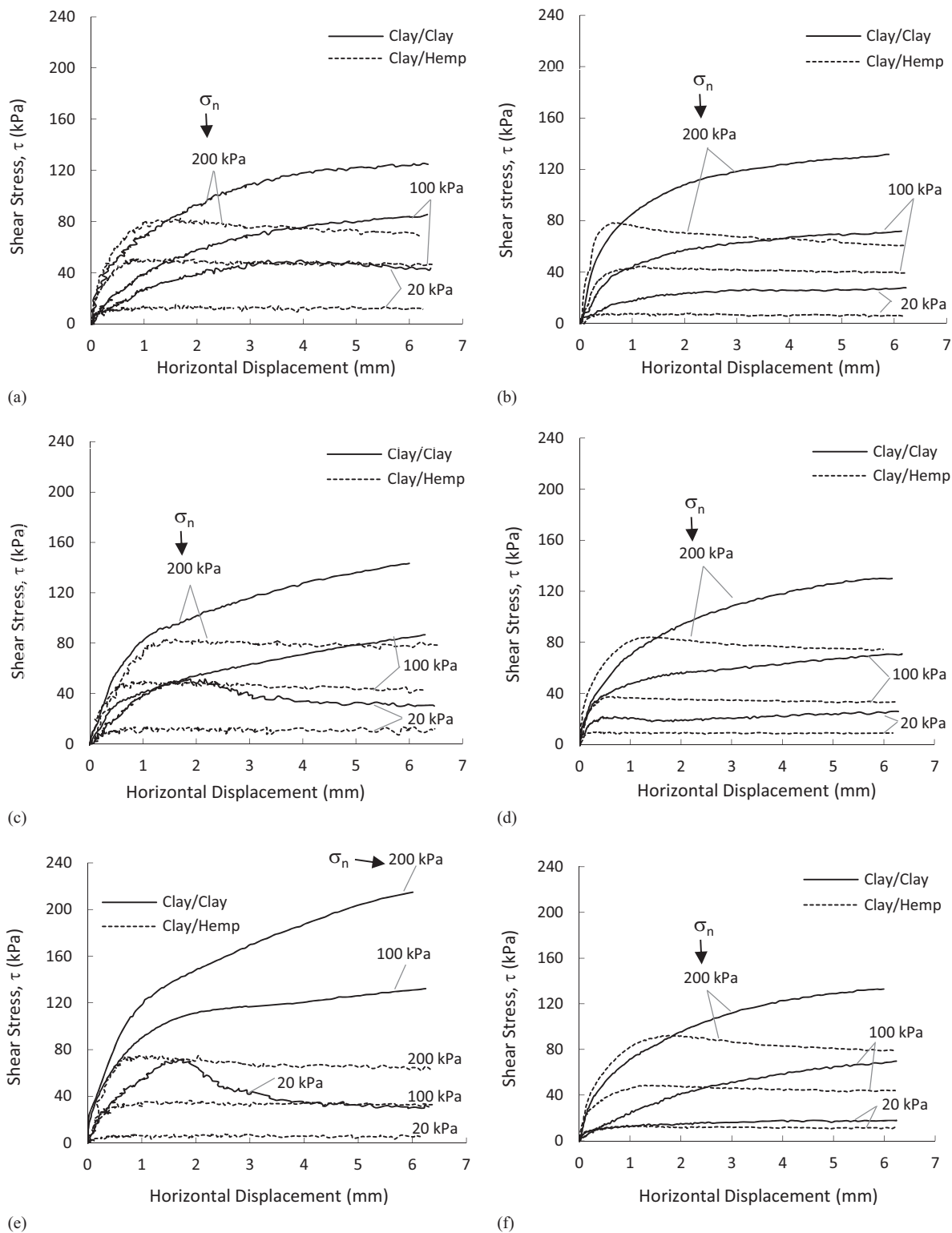


Fig. 7. Variation of shear stress with horizontal displacement in undrained (unconsolidated, quick) and drained (consolidated, slow) direct shear tests: (a) undrained, $w = 20\%$; (b) drained, $w = 20\%$; (c) undrained, $w = 18\%$; (d) drained, $w = 18\%$; (e) undrained, $w = 14\%$; and (f) drained, $w = 14\%$.

$w = 14\%$ exhibited the highest shear strength despite the fact that it had the smallest dry density. This indicates that the initial matric suction (rather than dry density) may have dominated the undrained shear strength of the clay.

The maximum shear stresses measured in the consolidated drained clay–clay tests are presented in Fig. 8(b). In these tests, the

specimens were given access to water, allowed to consolidate under σ_n , and sheared at a slow rate to facilitate drainage. Unlike the as-compacted undrained tests, the maximum shear stresses were governed by the applied consolidation stress and were relatively insensitive to the compaction water content. A comparison with the results of the as-compacted “unsaturated” tests indicated that the

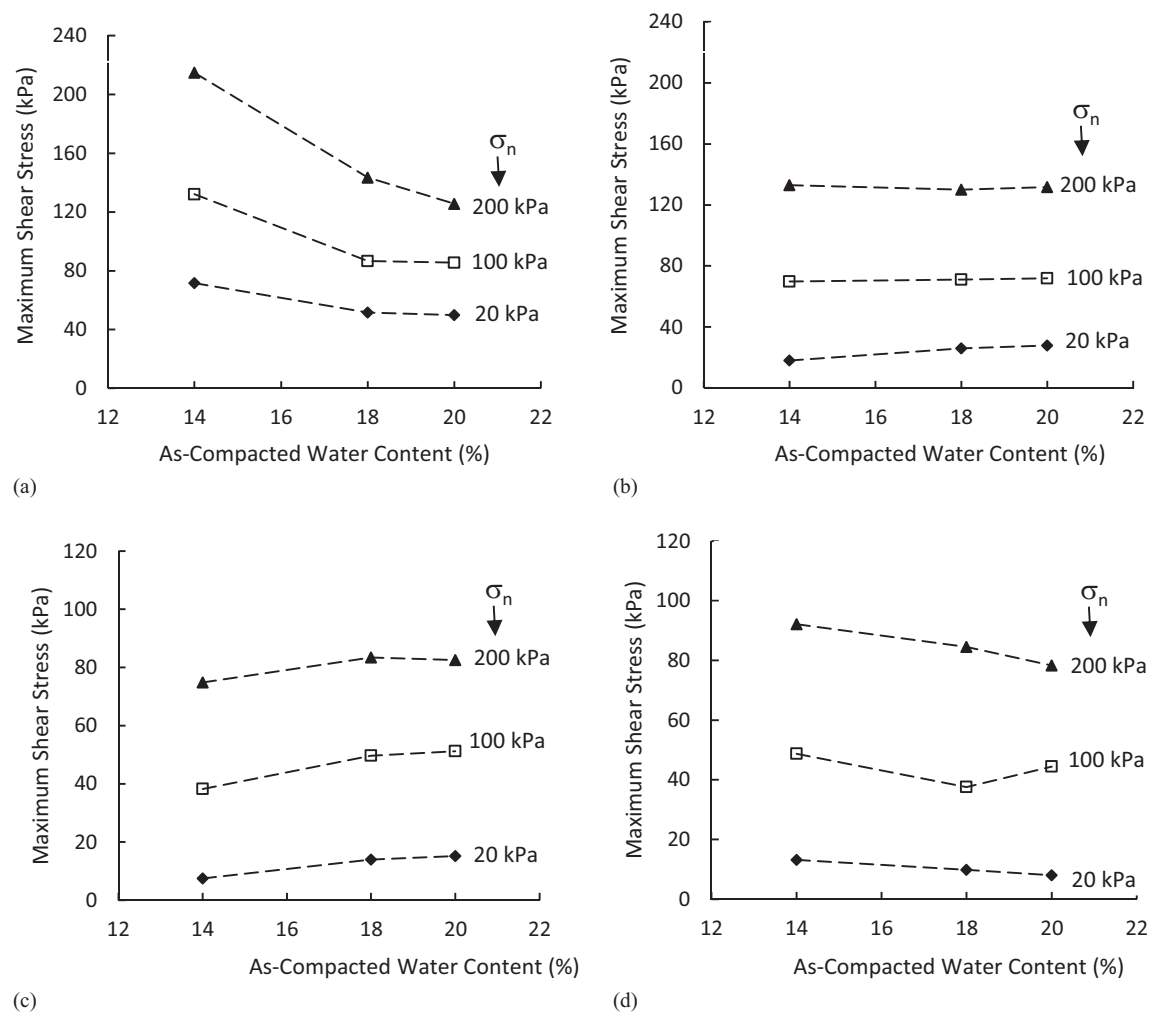


Fig. 8. Variation of maximum shear stress with water content for (a) undrained clay-clay; (b) drained clay-clay; (c) undrained clay-hemp; and (d) drained clay-hemp tests.

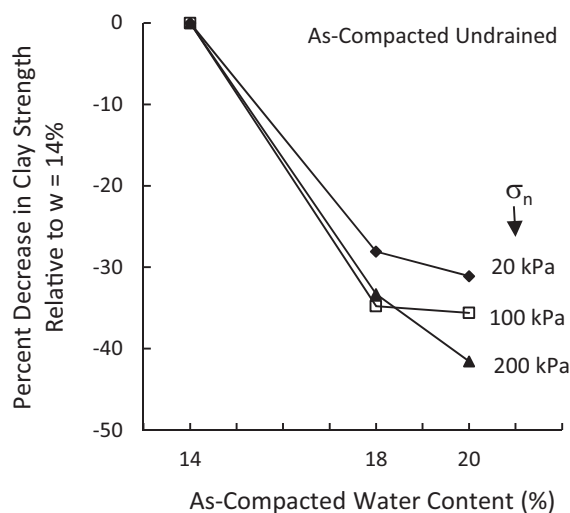


Fig. 9. Effect of compaction water content on the clay-clay direct shear strength.

maximum shear stress for any given water content and applied normal stress was larger for the unconsolidated “undrained” tests. Moreover, the differences between the drained and “undrained”

shear stresses increased as the compaction water content decreased from 20 to 14% and as the applied normal stress decreased from 200 to 20 kPa. A factor λ is defined as the ratio of the “undrained” to “drained” maximum shear stress at a given compaction water content and normal stress. The calculated values of λ are found to be approximately equal to 1.0 for $w = 20\%$ and $\sigma_n = 200$ kPa, increasing to values as high as $\lambda \approx 4$ for $w = 14\%$ and $\sigma_n = 20$ kPa.

Unlike the as-compacted quick “clay-clay” results that reflected a decreasing trend of maximum shear stress with increasing compaction water content, the quick interface “clay-hemp” [Fig. 8(c)] tests indicated an opposite trend whereby specimens that are dry of optimum ($w = 14\%$) exhibited the lowest interface shear stresses. As an example, the maximum interface clay-hemp stress increased from 7.4 to 15.1 kPa (for $\sigma_n = 20$ kPa) as the compaction water content increased from 14 to 20%. A similar increase (from 74.8 to 82.5 kPa) was witnessed for the case with $\sigma_n = 200$ kPa. This trend contradicts findings from published interface direct shear tests between unsaturated compacted clays and geosynthetics.

Ellithy and Gabr (2000) reported a drop of 64% in the interface strength between as-compacted kaolinite and a rough geomembrane when the water content was increased from 28 to 32%. Abu-Farsakh et al. (2007) reported that the interface shear strength between two soils and a geogrid decreased by an average of 34% (from dry of optimum to optimum) and 56% (dry of optimum to wet

of optimum) for a CL-ML soil and decreased by an average of 16% and 52%, respectively for a CL soil. Seed and Boulanger (1991) reported that the interface shear strength between smooth high-density polyethylene and as-compacted clay was higher for samples compacted at lower water contents, concluding that a major transition in interface strength occurs at high water contents and degrees of saturation. Finally, Hatami and Esmaili (2015) stated that reductions of up to 60–70% in the interface shear strength have been reported at higher compaction water contents, particularly in marginal soils with considerable fines content.

It is hypothesized that the unexpected small clay–hemp interface shear stresses that were measured with the as-compacted unsaturated specimens (particularly at $w = 14\%$) in the quick shearing tests could be due to partial local drainage (exchange of water) at the level of the interface between the clay and hemp. An investigation of the internal structure and composition of a hemp fiber using SEM (Fig. 10) indicated that each individual fiber comprised a number of smaller fibers that are separated by an internal void structure, forming drainage conduits that could facilitate drainage of water from the thin clay surface that is in contact with the hemp fibers. The fact that the soil included 45% sand in its composition could facilitate this interaction at the fiber–soil interface (Fig. 2). The stimulus for any local water exchange could be the hydraulic gradient resulting from the application of the normal stress or the generation of pore water pressure during shear.

If such local exchange of water occurs, it could increase the water content and degree of saturation locally at the interface resulting in partial or complete loss of matric suction, form a film of water at the interface that could enhance soil sliding and reduce the interface strength, and/or reduce potential generation of negative pore

water pressure (for small w and σ_n) or increase the potential generation of positive pore pressure (for high w and σ_n) during undrained shear (Jones and Dixon 1998; Fleming et al. 2006; Abu-Farsakh et al. 2007). Any partial drainage or local exchange of water at the interface could thus prohibit the interface material (hemp in this case) from mobilizing the full undrained shear strength of the clay that is in contact with it. Drainage at interfaces between soils and solids was discussed by Miller and Hamid (2007), who detected a decrease of water content in clay during interface shearing due to the disruption of the menisci between soil particles causing a decrease in matric suction.

The fact that the maximum interface shear stress measured in the case of $w = 14\%$ (lowest dry density) is consistently smaller than the shear stress measured for $w = 18$ and 20% (higher dry density) indicates that the initial dry density could have played a role in defining the interface shear resistance in quick interface direct shear tests. The hypothesized loss of matric suction at the interface due to possible local drainage may have unmasked the expected positive correlation between dry density and the interface shear resistance.

The hypothesis of partial/local drainage at the interface in fast as-compacted clay–hemp direct shear tests is supported by the results of the consolidated drained interface tests presented in Fig. 8(d). A comparison between the as-compacted unsaturated tests and the consolidated drained tests indicates that the difference in the clay–hemp interface response was generally small [Figs. 8(c and d)]. At the driest water content of 14%, the interface resistance was slightly lower ($\sim 25\%$ lower on average) in the undrained tests, whereas the opposite is true (undrained strength 25% higher on average) for the cases with $w = 18$ and 20% . The differences observed in the clay–hemp interface strength in the two types of tests are

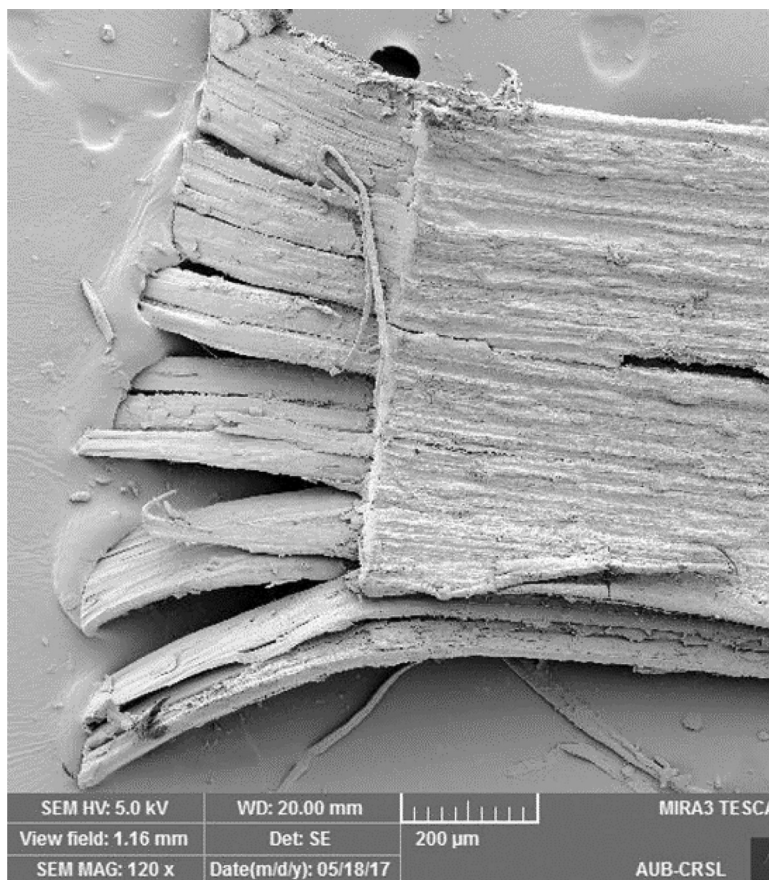


Fig. 10. Internal structure of hemp fibers (120 \times magnification).

considered small compared with the differences observed in clay–clay tests where the ratio of the “undrained” to “drained” maximum shear stress reached a value of 4 for $w = 14\%$ and $\sigma_n = 20$ kPa. These observations support the hypothesis of local drainage/wetting of the interface between the hemp and the soil in as-compacted interface direct shear tests.

Pullout Tests

The maximum pullout stresses that were measured in the pullout tests are presented in Fig. 11. Failure was observed to occur by sudden slippage. Although continuous measurements of the displacement (due to slip) of the fiber were not targeted, an estimate of the overall horizontal displacement prior to slippage was obtained by monitoring the displacement of a mark that was placed on the cable that was used to pull the embedded fiber. The ultimate pullout stress was calculated as the ratio of the force needed to pull out the fiber to the corrected contact area between the fiber and the compacted clay. Given the cross-sectional area, short length, and relatively high modulus of elasticity of the fiber, the shear stress could be assumed to be uniform along the fiber length, with potential progressive failure at the interface being highly unlikely.

Maximum Pullout Stress versus Compaction Water Content

Results of the pullout tests in Fig. 11 indicate that for fibers that were pulled out at a fast rate in as-compacted specimens, the maximum stresses were larger than the stresses observed in identical slow pullout tests on clay that was allowed to consolidate in the presence of water. These results indicate that unlike fast interface direct shear tests, where partial drainage could have occurred at the level of the interface and reduced the interface strength, fast single fiber pullout tests seem to have mobilized a significant percentage of the “undrained” shear strength of the compacted clay. This hypothesis is reinforced by the observed relationship between the measured pullout stresses and the compaction water content [Fig. 11(b)] in which significant reduction in the pullout stress is observed as the water content was increased from 14 to 18% and 20% in fast pullout tests. A comparison between the results of the fast fiber pullout tests [Fig. 11(b)] and the fast direct shear clay–clay tests [Fig. 8(a)] shows remarkable consistency with regard to the variation of the maximum clay–clay shear stresses and ultimate pullout stresses with the compaction water content. The pullout stresses decreased by about 33–36% (depending on the applied normal stress) when the as-compacted water content increased from 14 to 18% and from 28 to 40% when the water content was increased to 20%. These percentages are comparable to the percentage decreases in clay–clay strength from fast direct shear tests (Fig. 9). This observation further reinforces the hypothesis of a true “undrained” behavior in the single fiber pullout tests.

Similar reductions in the maximum pullout stress with compaction water content were reported by Tang et al. (2010) for “undrained” single fiber pullout tests using polypropylene fibers and a CL soil, in Jamie et al. (2013) for single fiber pullout tests using sisal fibers and a natural clay ($PI = 15\%$), and in Hatami and Esmaili (2015) for fast small-scale pullout tests using a geotextile and three clayey soils (SC, CL-ML, and CL). In the tests reported by Tang et al. (2010), the peak pullout stress was observed to decrease by about 18% when the compaction water content was increased from 14.5 to 20.5% (optimum water content is 16.5%). Tang et al. (2010) attributed this drop to a decrease in capillarity force and effective stress between particles at the interface and to the lubricating role that water could play at the interface, resulting in a decrease in interfacial friction. In the tests reported by Jamie et al. (2013), reductions of approximately 45–55% were observed

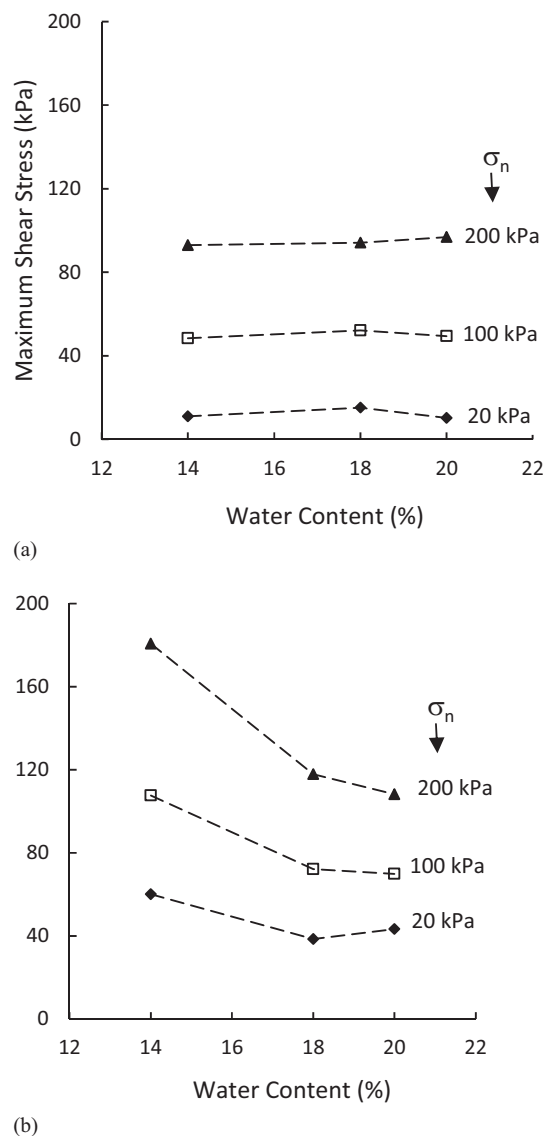


Fig. 11. Maximum pullout stress versus water content for (a) slow rate pullout (consolidated drained); and (b) fast rate pullout tests (as-compacted quick).

in the pullout strength as the saturation of specimens was increased from ~60 to 95%. In tests by Hatami and Esmaili (2015), reductions of approximately 36–46% were observed in the pullout strength when the water content was increased from 2% dry of optimum to 2% wet of optimum. It should be noted that the applied normal stress did not have a significant effect on the percentage decrease in pullout resistance at larger water contents, as indicated in the tests reported by Jamie et al. (2013) and Hatami and Esmaili (2015). This also applies to the fast hemp pullout tests conducted in the present study.

Unlike the fast pullout tests on as-compacted specimens, the results of the consolidated “drained” pullout tests were largely insensitive to the initial compaction water content and highly sensitive to the applied consolidation pressure [Fig. 11(a)]. This is in line with the results observed in the consolidated drained interface direct shear tests. In consolidated drained tests, the maximum pullout stress was expected to be relatively insensitive to the initial water content because the specimens were allowed to exchange water with the surrounding water bath during consolidation and fiber

pullout. As a result, the interface between the hemp and the soil was expected to become lubricated and the effect of matric suction at the interface to become minimal, irrespective of the initial water content.

Effect of Normal Stress on the Maximum Pullout Stress

The variation of the hemp–clay maximum pullout stress with applied normal stress is presented in Fig. 12. Results indicate that the maximum pullout stress increases linearly with applied normal pressure, irrespective of the test type. These results are in line with findings from published studies (e.g., Jamie et al. 2013; Zhang et al. 2014, 2015, 2016; Hatami and Esmaili 2015; Zhu et al. 2015) that investigated the effect of the applied normal stress on the pullout resistance between single fibers and soils.

The positive correlation between normal stress and pullout resistance has been explained by several authors. Zhu et al. (2015) stated that at a relatively low confining pressure, the contact between the soil and the fiber is loose and characterized by many voids at the interface. As a result, the real contact area is grossly overestimated by the theoretical area. At a higher confining pressure, better bonding between the fiber and the surrounding soil is ensured with a reduction in the voids and an increase in the contact area at the soil–fiber interface. In addition, at low confinement, pullout will result in rotation and rearrangement of the soil particles at the interface. This is significantly reduced at higher confining pressures. Enhancing confinement will lead to a better deformation–compatibility between the fiber and the soil. Zhang et al. (2015) hypothesized based on results from optical microscopy images that the higher the confining pressure, the more interlocked or interbonded the soil particles are and that more particles will probably penetrate the fiber surface, causing indentations and roughening along the fiber surface. The possibility of angular hard bodies (like sands) causing plastic deformations to a fiber body at higher compaction loads or normal stresses was also reported by Tang et al. (2010) who investigated the interface morphologies of fiber-reinforced soils using SEM. They observed that after pullout some soil particles were attached to the fiber surface, indicating that the interfacial soil structure had been disturbed or even broken during the shear process.

Results in Fig. 12 indicate that at the lowest normal stress adopted in the present study ($\sigma_n = 20$ kPa), the maximum pullout stresses varied between 39 kPa ($w = 20\%$) and 60 kPa ($w = 14\%$) for the as-compacted quick tests and 10 to 15 kPa for the consolidated drained tests. The relatively large pullout stresses observed in the as-compacted quick tests for the low confining pressure of 20 kPa can be attributed to the effect of matric suction. As the normal stress was increased to 100 and 200 kPa, the pullout stresses increased linearly, reflecting an improved deformation–compatibility between the fiber and the soil and better interlocking or interbonding between the soil particles and the hemp fiber.

It should be noted that in all the as-compacted quick pullout tests that were conducted in the present study, a visual inspection of the fiber after pullout showed particles of clay that were bonded to the fiber. This observation could lead to the conclusion that the failure surface in as-compacted quick pullout tests may not have been confined to the hemp–clay interface but that it could have migrated into the overlying and underlying clay. This could explain the differences in the shear stresses observed in the as-compacted quick pullout tests and the as-compacted quick interface direct shear tests. It could be concluded that confining a single hemp fiber within a clay specimen from all directions (pullout test setup) may have resulted in enhanced fiber–soil interaction by preserving the matric suction at the interface, minimizing drainage/wetting at the interface, and

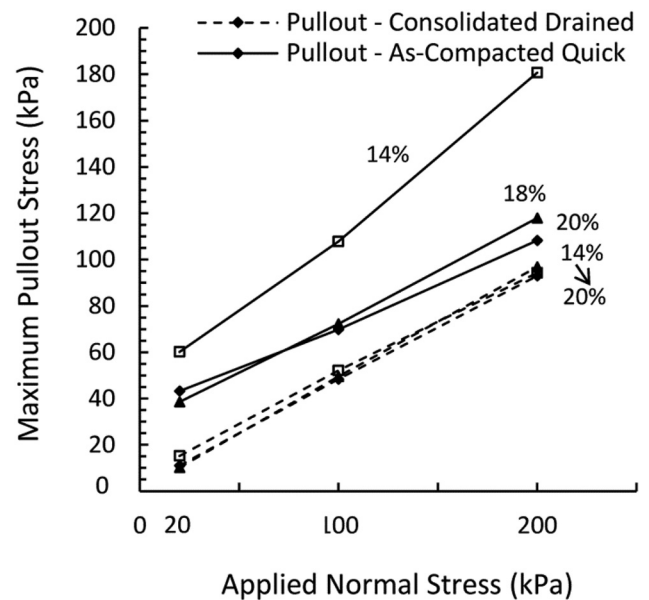


Fig. 12. Effect of applied normal stress on maximum pullout stress.

allowing the rough hemp fiber to mobilize the undrained shear strength of the surrounding clay in an efficient manner.

Interface Shear Strength

The maximum shear stresses that were measured in the direct shear tests are plotted with the results of the maximum single fiber pullout tests in Fig. 13. The clay–clay failure envelopes act as a reference because the envelopes represent an upper bound for any interface shear or pullout resistance. The resulting Mohr–Coulomb failure envelopes for both the clay–clay and clay–interface tests and their associated shear strength parameters are shown in Fig. 13 and in Table 3 for comparison.

Results in Fig. 13 indicate that the natural compacted clay exhibited c' and ϕ' values ranging from 5.4 to 14.4 kPa and 27.1 to 29.4°, respectively, as indicated by the consolidated drained direct shear tests. These results could be considered realistic given the fact that the clay has more than 45% sand in its composition. When the clay was tested in an unconsolidated state and using a fast rate of loading, the total stress shear strength parameters c and ϕ were found to range from 38.6 to 54.5 kPa and 20.5 to 35°, respectively. The relatively large apparent cohesion is expected for as-compacted clay specimens that are sheared under undrained conditions. The higher than anticipated undrained friction angle could only be explained by the unsaturated state of the specimens and the presence of a significant fraction of sand in the clay.

With regard to the clay–hemp interface shear strength parameters, results in Fig. 13(a) indicate that, for slow drained interface direct shear tests and slow rate pullout tests, the failure envelopes are close to each other. The drained interface friction angles pertaining to the slow rate pullout tests ranged from $\delta' = 23.7$ to 25.6° and were slightly but consistently larger (by 1 to 3°) than δ' for interface direct shear tests. Similar observations were reported by Alfaro et al. (1995) where frictional interface properties from pullout tests were found to be higher than those determined from direct shear tests. The interface friction angles are lower than the drained friction angle of the clay ($\phi' = 27.1$ to 29.4°), indicating an interface friction efficiency that is in the range of 80–85%. The effective interface cohesive intercepts (a') were found to be small, ranging

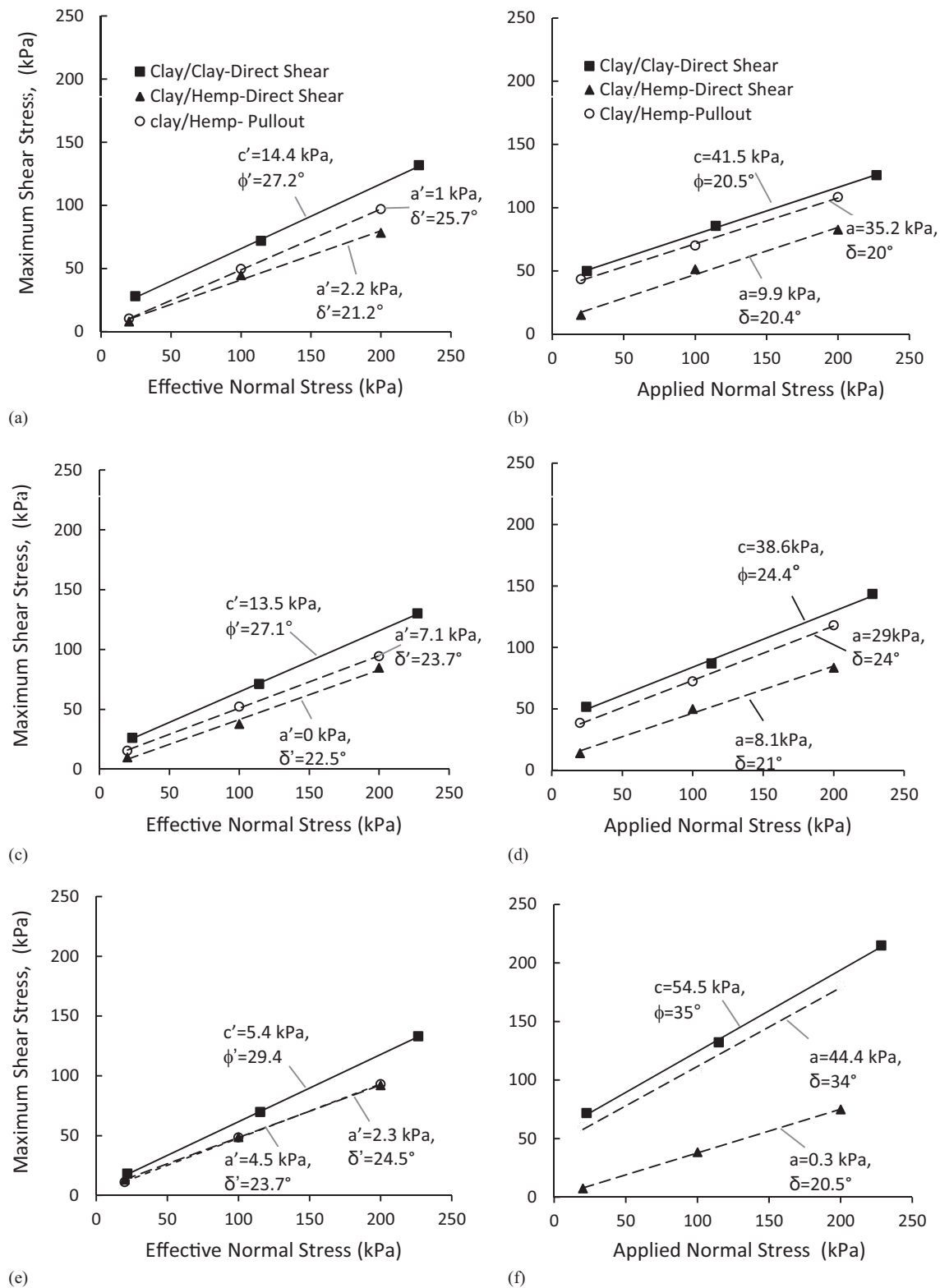


Fig. 13. Comparison between results of drained (consolidated, slow) and undrained (unconsolidated, quick) direct shear and single fiber pullout tests: (a) drained, $w = 20\%$; (b) undrained, $w = 20\%$; (c) drained, $w = 18\%$; (d) undrained, $w = 18\%$; (e) drained, $w = 14\%$; and (f) undrained, $w = 14\%$.

from 0 to 4.5 kPa for the direct shear tests and 1.0 to 7.1 kPa for pull-out tests.

On the other hand, the interface parameters pertaining to the unconsolidated fast tests indicate a superior interface response for the single fiber pullout tests. The improved interface pullout response is exhibited clearly in the adhesion intercept (average

$a = 36$ kPa), which was much larger than that of the fast interface direct shear tests (average $a = 6.0$ kPa). The “adhesion” in the fast pullout tests constituted around 75% of the “cohesion” observed in the fast clay–clay direct shear tests, reinforcing the hypothesis that the fast pullout tests are more reflective of “undrained” interface behavior. These results are important and

Table 3. Adhesion and interface friction angle for direct shear and fiber pullout

Water content (%)	Slow/drained test				Fast/undrained test			
	Direct shear		Fiber pullout		Direct shear		Fiber pullout	
	a' (kPa)	δ' (degrees)	a' (kPa)	δ' (degrees)	a (kPa)	δ (degrees)	a (kPa)	δ (degrees)
14	4.5	23.7	2.3	24.5	0.3	20.5	44.4	34.0
18	0	22.5	7.1	23.7	8.1	21.0	29.0	24.0
20	2.2	21.2	1.0	25.6	9.9	20.4	35.2	20.0

indicate that interface direct shear tests may not be representative of the true interface response for short-term stability conditions involving rapid loading for the hemp–soil interface investigated in the present study.

Discussion and Relevance of Results

The realistic and accurate evaluation of soil–fiber interface properties is key for reliable and sustainable design of fiber-reinforced soil structures. Numerous studies in the past have investigated the soil–geosynthetic interface properties and interaction mechanisms using pullout and interface shear tests.

From a practical standpoint, direct shear and pullout test results could be used to recommend design values for the interface parameters required to predict the response of the natural clay that is tested in the present study when reinforced with natural hemp fibers. The interface parameters constitute necessary input to any predictive model for fiber-reinforced clay (e.g., Zornberg 2002; Jamie et al. 2013; Nguyen and Fatahi 2016; Mirzababaei et al. 2018b) and are generally described using interface coefficients $C_{i,c}$ and $C_{i,\phi}$, where $C_{i,c}$ represents the ratio of the fiber–clay adhesion to the clay–clay cohesion ($C_{i,c} = a/c$) and $C_{i,\phi}$ represents the ratio of the interface friction coefficient to the clay–clay friction coefficient ($C_{i,\phi} = \tan\delta'/\tan\phi$).

Due to partial drainage considerations at the interface, results from interface direct shear tests can only be used reliably to estimate the interface coefficients for consolidated drained conditions. As such, only the drained $C_{i,\phi}$ was calculated from interface direct shear tests and compared with $C_{i,\phi}$ from drained single fiber pullout tests in Fig. 14(a). For the direct shear tests, an average drained interface coefficient $C_{i,\phi} \approx 0.78$ was obtained with minimum sensitivity to the compaction water content. For the single fiber pullout tests, the average $C_{i,\phi}$ was 0.85. Given the relatively small values of adhesion that were obtained in the drained interface direct shear and pullout tests, it could be conservatively assumed that the drained cohesive interface coefficient $C_{i,c}$ is equal to zero in characterizing the drained interface behavior.

For compacted fiber-reinforced clay systems that are governed by long-term stability conditions (such as compacted fiber-reinforced slopes and embankments), the drained interface friction coefficient between the fiber and the clay constitutes a necessary input for design. Results of the present study show that the drained interface strength could be measured reliably in a laboratory setting using small-scale direct shear or single fiber pullout tests. In field applications, the characteristics of the internal structure of fiber-reinforced clays (randomly distributed discrete fibers in a clay matrix) and the expected mode of failure that is generally governed by pullout of fibers across potential shear planes lead to the conclusion that results from single fiber pullout tests may better represent the response of the hemp–soil interface. For the natural hemp fibers and the natural CL clay in the present study, the drained interface strength can thus be described by the interface friction coefficient

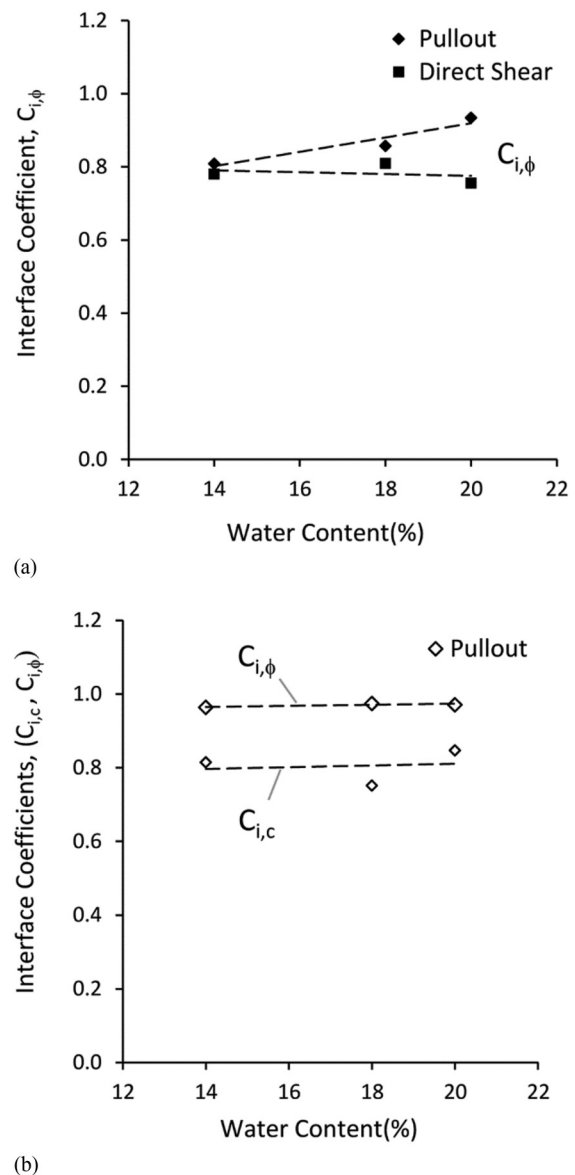


Fig. 14. Interface coefficients from direct shear and pullout tests: (a) slow (consolidated drained); and (b) fast (unconsolidated undrained).

$C_{i,\phi}$, which can conservatively be assigned a value of 0.82, representing the average between interface direct shear and single fiber pullout tests.

For compacted fiber-reinforced clay systems that are governed by short-term stability, the interface coefficients that correspond to “unconsolidated undrained” loading conditions are expected to be more representative of the as-compacted response of the composite.

Under such conditions, results from the experimental program indicate that interface interaction coefficients may be best quantified using the results of the fast single fiber pullout tests. The resulting interface coefficients are plotted in Fig. 14(b) and indicate that the “undrained” $C_{i,c}$ and $C_{i,\phi}$ are relatively insensitive to the compaction water content with average values of 0.75 and 0.98, respectively.

It is worth noting that the calculated interface coefficients between hemp and clay for drained and undrained conditions could be considered to be relatively high and insensitive to the compaction water content. The relatively high interface coefficients can be attributed to the relatively high surface roughness of the hemp fibers and to the presence of a significant portion of sand within the clay matrix. The relatively higher interface coefficients for hemp are encouraging and indicative of a potentially effective soil–fiber interaction, particularly with natural soils that include a wide range of grain sizes in their gradation. On the other hand, the insensitivity of the coefficients to the water content is indicative of a proportionality between the shear strength of the clay and the maximum interface shear stress. For consolidated drained tests, the maximum shear stresses in both clay–clay and clay–hemp tests exhibited minimal sensitivity to the compaction water content. As a result, the interface coefficients were also relatively insensitive to the water content.

It should be noted that the clay–hemp interface behavior (especially from pullout tests) is best described using concepts of mechanical compatibility between the clay and the hemp. In fact, several interface mechanical models that focus on the shear stress versus displacement relationship exist in the literature for single fiber pullout tests. Examples of mechanical compatibility models that model the multistage pullout versus displacement relationships are presented by Zhu et al. (2014) for pullout tests on polypropylene fibers embedded in a silty clay and by Zhang et al. (2014, 2015, 2016) and Zhu et al. (2015) for pullout tests on optic fibers and an SP soil.

Conclusions

In this paper, direct shear interface tests and single fiber pullout tests were conducted in a consolidated drained setup and an “unconsolidated undrained” setup to characterize the interface resistance between natural hemp fibers and natural CL clay that contained 45% sand in its composition. Based on the results, the following observations can be made:

- Minimal differences between drained and “undrained” interface response were observed for interface tests conducted using the direct shear setup. This small difference was attributed to possible partial drainage/wetting that occurred at the level of the interface through the hemp surface that was prepared by gluing individual fibers on a steel plate. This partial drainage could have prevented the hemp from mobilizing a “true” undrained interface resistance between the clay and the interface.
- In tests where the fiber was pulled out at a fast rate from as-compacted specimens, the ultimate pullout resistance was larger than that of tests where the fiber was pulled out slowly from consolidated specimens. This indicates that “undrained” behavior with minimal loss of matric suction may have been exhibited in fast rate pullout tests, which allowed the interface resistance to benefit from the relatively high undrained strength of the clay.
- The effective drained interface resistance between hemp and the clay tested in the present study could be realistically defined from either pullout or direct shear tests and is

characterized by an interface friction angle δ' that ranges between 22.5 and 23.7° in the direct shear tests and between 23.7 and 25.7° in pullout tests. These values correspond to average drained interface friction coefficients $C_{i,\phi}$ of 0.78 (direct shear) and 0.85 (pullout).

- For the undrained response, the interface parameters obtained from the single fiber pullout tests were found to be more reliable and are characterized by interface coefficients $C_{i,c}$ and $C_{i,\phi}$ of 0.75 and 0.98, respectively.

Finally, it is worth noting that hemp fibers have a high water-absorption capacity that may affect the fiber–clay interface interaction. The tests in the present study were limited to two extreme conditions of short-term undrained loading (water content is more or less fixed) and long-term consolidated drained loading where test specimens are exposed to water throughout the stages of the test. Tests could be conducted in the future to investigate the effect of hemp water absorption on the mechanics of the interface interaction.

Acknowledgments

The authors would like to acknowledge the support of the American University of Beirut (AUB) University Research Board and the Lebanese National Council for Scientific Research in supporting the research of the authors.

References

- Abou Diab, A., S. S. Najjar, S. Sadek, H. Taha, H. Jaffal, and M. Alahmad. 2018. “Effect of compaction method on the undrained strength of fiber-reinforced clay.” *Soils Found.* 58 (2): 462–480. <https://doi.org/10.1016/j.sandf.2018.02.013>.
- Abou Diab, A., S. Sadek, S. Najjar, and M. H. Abou Daya. 2016. “Undrained shear strength characteristics of compacted clay reinforced with natural hemp fibers.” *Int. J. Geotech. Eng.* 10 (3): 263–270. <https://doi.org/10.1080/19386362.2015.1132122>.
- Abu-Farsakh, M., J. Coronel, and M. Tao. 2007. “Effect of soil moisture content and dry density on cohesive soil-geosynthetic interactions using large direct shear tests.” *J. Mater. Civil Eng.* 19 (7): 540–549. [https://doi.org/10.1061/\(ASCE\)0899-1561\(2007\)19:7\(540\)](https://doi.org/10.1061/(ASCE)0899-1561(2007)19:7(540)).
- Alfaro, M., N. Miura, and D. Bergado. 1995. “Soil-geogrid reinforcement interaction by pullout and direct shear tests.” *Geotech. Test. J.* 18 (2): 157–167. <https://doi.org/10.1520/GTJ10319J>.
- Bacas, B. M., J. Cañizal, and H. Konietzky. 2015. “Frictional behavior of three critical geosynthetic interfaces.” *Geosynth. Int.* 22 (5): 355–365. <https://doi.org/10.1680/jgein.15.00017>.
- Bosscher, P. J., and G. C. Ortiz. 1987. “Friction properties between sand and various construction materials.” *Int. J. Geotech. Eng.* 113 (9): 1035–1039. [https://doi.org/10.1061/\(ASCE\)0733-9410\(1987\)113:9\(1035\)](https://doi.org/10.1061/(ASCE)0733-9410(1987)113:9(1035)).
- Bouhicha, M., F. Aouissi, and S. Kenai. 2005. “Performance of composite soil reinforced with barley straw.” *Cem. Concr. Compos.* 27 (5): 617–621. <https://doi.org/10.1016/j.cemconcomp.2004.09.013>.
- Cardile, G., N. Moraci, and L. S. Calvarano. 2016. “Geogrid pullout behavior according to the experimental evaluation of the active length.” *Geosynth. Int.* 23 (3): 194–205. <https://doi.org/10.1680/jgein.15.00042>.
- Dittenber, D. B., and H. V. S. GangaRao. 2012. “Critical review of recent publications on use of natural composites in infrastructure.” *Comp. Part A* 43 (8): 1419–1429. <https://doi.org/10.1016/j.compositesa.2011.11.019>.
- Ellithy, G. S., Gabr, M. A. 2000. “Compaction moisture effect on geomembrane/clay interface shear strength.” In *Proc., Conf. on Advances in Transportation and Geoenvironmental Systems Using Geosynthetics*, Geotechnical Special Publication 103, edited by J. C. Zornberg and B. R. Christopher, 39–53. Reston, VA: ASCE.
- Fan, M. 2010. “Characterization and performance of elementary hemp fibres: Factors influencing tensile strength.” *Bioresources* 5 (4): 2307–2322.

- Ferreira, F. B., C. S. Vieira, and M. L. Lopes. 2015. "Direct shear behaviour of residual soil–geosynthetic interfaces—Influence of soil moisture content, soil density and geosynthetic type." *Geosynth. Int.* 22 (3): 257–272. <https://doi.org/10.1680/gein.15.00011>.
- Fleming, I. R., J. S. Sharma, and M. B. Jogi. 2006. "Shear strength of geomembrane–soil interface under unsaturated conditions." *Geotext. Geomembr.* 24 (5): 274–284. <https://doi.org/10.1016/j.geotextmem.2006.03.009>.
- Gan, J. K. M., D. G. Fredlund, and H. Rahardjo. 1988. "Determination of the shear strength parameters of an unsaturated soil using the direct shear test." *Can. Geotech. J.* 25 (38): 500–510. <https://doi.org/10.1139/t88-055>.
- Hatami, K., and D. Esmaili. 2015. "Unsaturated soil–woven geotextile interface strength properties from small-scale pullout and interface test." *Geosynth. Int.* 22 (2): 161–172. <https://doi.org/10.1680/gein.15.00002>.
- Hejazi, S. M., M. Sheikhzadeh, S. M. Abtahi, and H. Zadhoush. 2012. "A simple review of soil reinforcement by using natural and synthetic fibers." *Constr. Build. Mater.* 30 (May): 100–116. <https://doi.org/10.1016/j.conbuildmat.2011.11.045>.
- Hossain, B., Z. Hossain, and T. Sakai. 2012. "Interaction properties of geosynthetic with different backfill soils." *Int. J. Geosci.* 3 (5): 24938. <https://doi.org/10.4236/jgg.2012.35104>.
- Jamie, M., P. Villard, and H. Guiras. 2013. "Shear failure criterion based on experimental and modeling results for fiber-reinforced clay." *Int. J. Geomech.* 13 (6): 882–893. [https://doi.org/10.1061/\(ASCE\)GM.1943-5622.0000258](https://doi.org/10.1061/(ASCE)GM.1943-5622.0000258).
- Jewell, R. A., and C. P. Wroth. 1987. "Direct shear tests on reinforced sand." *Géotechnique* 37 (1): 53–68. <https://doi.org/10.1680/geot.1987.37.1.53>.
- Jones, D. R. V., and N. Dixon. 1998. "Shear strength properties of geomembrane/geotextile interfaces." *Geotext. Geomembr.* 16 (1): 45–71. [https://doi.org/10.1016/S0266-1144\(97\)10022-X](https://doi.org/10.1016/S0266-1144(97)10022-X).
- Khoury, C. N., G. A. Miller, and K. Hatami. 2011. "Unsaturated soil–geotextile interface behavior." *Geotext. Geomembr.* 29 (1): 17–28. <https://doi.org/10.1016/j.geotextmem.2010.06.009>.
- Kishida, H., and M. Uesugi. 1987. "Tests of the interface between sand and steel in the simple shear apparatus." *Géotechnique* 37 (1): 45–52. <https://doi.org/10.1680/geot.1987.37.1.45>.
- Koerner, R. M., J. P. Martin, and G. R. Koerner. 1986. "Shear strength parameters between geomembranes and cohesive soils." *Geotext. Geomembr.* 4 (1): 21–30. [https://doi.org/10.1016/0266-1144\(86\)90034-8](https://doi.org/10.1016/0266-1144(86)90034-8).
- Lemos, L. J. L., and P. R. Vaughan. 2000. "Clay–interface shear resistance." *Géotechnique* 50 (1): 55–64. <https://doi.org/10.1680/geot.2000.50.1.55>.
- Li, Z., X. Wang, and L. Wang. 2006. "Properties of hemp fibre reinforced concrete composites." *Compos. Part A* 37 (3): 497–505. <https://doi.org/10.1016/j.compositesa.2005.01.032>.
- Lin, D. G., B. S. Huang, and S. H. Lin. 2010. "3-D numerical investigations into the shear strength of the soil–root system of Makino bamboo and its effect on slope stability." *Ecol. Eng.* 36 (8): 992–1006. <https://doi.org/10.1016/j.ecoleng.2010.04.005>.
- Lu, M., H. Jing, Y. Zhou, and K. Xie. 2017. "General analytical model for consolidation of stone column-reinforced ground and combined composite ground." *Int. J. Geomech.* 17 (6): 04016131. [https://doi.org/10.1061/\(ASCE\)GM.1943-5622.0000836](https://doi.org/10.1061/(ASCE)GM.1943-5622.0000836).
- Maher, M. H., and D. H. Gray. 1990. "Static response of sands reinforced with randomly distributed fibers." *Int. J. Geotech. Eng.* 116 (11): 1661–1677. [https://doi.org/10.1061/\(ASCE\)0733-9410\(1990\)116:11\(1661\)](https://doi.org/10.1061/(ASCE)0733-9410(1990)116:11(1661)).
- Miller, G., and T. Hamid. 2007. "Interface direct shear testing of unsaturated soil." *Geotech. Test. J.* 30 (3): 182–191. <https://doi.org/10.1520/GTJ13301>.
- Mirzababaei, M. A., A. Arulrajah, A. Haque, S. Nimbalkar, and A. Mohajerani. 2018a. "Effect of fiber reinforcement on shear strength and void ratio of soft clay." *Geosynth. Int.* 25 (4): 471–480. <https://doi.org/10.1680/jgein.18.00023>.
- Mirzababaei, M., A. Arulrajah, S. Horpibulsuk, and M. Aldava. 2017. "Shear strength of a fibre-reinforced clay at large shear displacement when subjected to different stress histories." *Geotext. Geomembr.* 45 (5): 422–429. <https://doi.org/10.1016/j.geotextmem.2017.06.002>.
- Mirzababaei, M., M. Mohamed, A. Arulrajah, S. Horpibulsuk, and V. Anggraini. 2018b. "Practical approach to predict the shear strength of fibre-reinforced clay." *Geosynth. Int.* 25 (1): 50–66. <https://doi.org/10.1680/jgein.17.00033>.
- Najjar, S. S., S. Sadek, and H. Taha. 2014. "Use of hemp fibers in sustainable compacted clay systems." *Geo-Congress 2014 Technical Papers: Geo-Characterization and Modelling for Sustainability*, Geotechnical Special Publication 234, edited by M. Abu-Farsakh, X. Yu, and L. R. Hoyos, 1415–1424. Reston, VA: ASCE.
- Nguyen, L., and B. Fatahi. 2016. "Behaviour of clay treated with cement & fibre while capturing cementation degradation and fibre failure—C3F model." *Int. J. Plast.* 81 (Jun): 168–195. <https://doi.org/10.1016/j.iijplas.2016.01.015>.
- Ola, S. A. 1989. "Stabilization of lateritic soils by extensible fibre reinforcement." *Eng. Geol.* 26 (2): 125–140. [https://doi.org/10.1016/0013-7952\(89\)90002-1](https://doi.org/10.1016/0013-7952(89)90002-1).
- Paikowsky, S., C. Player, and P. Connors. 1995. "A Dual interface apparatus for testing unrestricted friction of soil along solid surfaces." *Geotech. Test. J.* 18 (2): 168–193. <https://doi.org/10.1520/GTJ10320J>.
- Prabakar, J., and R. S. Sridhar. 2002. "Effect of random inclusion of sisal fibre on strength behaviour of soil." *Constr. Build. Mater.* 16 (2): 123–131. [https://doi.org/10.1016/S0950-0618\(02\)00008-9](https://doi.org/10.1016/S0950-0618(02)00008-9).
- Punetha, P., P. Mohanty, and M. Samanta. 2017. "Microstructural investigation on mechanical behavior of soil–geosynthetic interface in direct shear test." *Geotext. Geomembr.* 45 (3): 197–210. <https://doi.org/10.1016/j.geotextmem.2017.02.001>.
- Seed, R. B., and R. W. Boulanger. 1991. "Smooth HDPE–clay liner interface shear strengths: Compaction effects." *Int. J. Geotech. Eng.* 117 (4): 686–693. [https://doi.org/10.1061/\(ASCE\)0733-9410\(1991\)117:4\(686\)](https://doi.org/10.1061/(ASCE)0733-9410(1991)117:4(686)).
- Soltani, A., A. Deng, and A. Taheri. 2018. "Swell–compression characteristics of a fiber–reinforced expansive soil." *Geotext. Geomembr.* 46 (2): 183–189. <https://doi.org/10.1016/j.geotextmem.2017.11.009>.
- Tang, C. S., J. Li, D. Y. Wang, and B. Shi. 2016. "Investigation on the interfacial mechanical behavior of wave-shaped fiber reinforced soil by pull-out test." *Geotext. Geomembr.* 44 (6): 872–883. <https://doi.org/10.1016/j.geotextmem.2016.05.001>.
- Tang, C. S., B. Shi, and L. Z. Zhao. 2010. "Interfacial shear strength of fiber reinforced soil." *Geotext. Geomembr.* 28 (1): 54–62. <https://doi.org/10.1016/j.geotextmem.2009.10.001>.
- Wang, H. 2002. "Design and optimization of chemical and mechanical processing of hemp for rotor spinning and textile applications". Ph.D. thesis, School of Materials Science and Engineering, Univ. of New South Wales.
- Wang, Y. X., P. P. Guo, F. Dai, X. Li, Y. L. Zhao, and Y. Liu. 2018. "Behavior and modeling of fiber reinforced clay under triaxial compression by using the combining superposition method with the energy-based homogenization technique." *Int. J. Geomech.* 18 (12): 04018172. [https://doi.org/10.1061/\(ASCE\)GM.1943-5622.0001313](https://doi.org/10.1061/(ASCE)GM.1943-5622.0001313).
- Wang, Y. X., P. P. Guo, W. X. Ren, B. X. Yuan, H. P. Yuan, Y. L. Zhao, S. B. Shan, and P. Cao. 2017. "Laboratory investigation on strength characteristics of expansive soil treated with jute fiber reinforcement." *Int. J. Geomech.* 17 (11): 04017101. [https://doi.org/10.1061/\(ASCE\)GM.1943-5622.0000998](https://doi.org/10.1061/(ASCE)GM.1943-5622.0000998).
- Wilson, S. D. 1970. "Suggested method of test for moisture–density relations of soils using Harvard compaction apparatus." In *Special Procedure for Testing Soil and Rock for Engineering Purposes*. 5th ed., 101–103. ASTM STP479. West Conshohocken, PA: ASTM.
- Zhang, C. C., H. H. Zhu, J. K. She, D. Zhang, and B. Shi. 2015. "Quantitative evaluation of optical fiber/soil interfacial behavior and its implications for sensing fiber selection." *IEEE Sens. J.* 15 (5): 3059–3067. <https://doi.org/10.1109/JSEN.2014.2386881>.
- Zhang, C. C., H. H. Zhu, and B. Shi. 2016. "Role of the interface between distributed fibre optic strain sensor and soil in ground deformation measurement." *Sci. Rep.* 6 (Nov): 36469. <https://doi.org/10.1038/srep36469>.
- Zhang, C. C., H. H. Zhu, B. Shi, and J. K. She. 2014. "Interfacial characterization of soil-embedded optical fiber for ground deformation measurement." *Smart Mater. Struct.* 23 (9): No. 095022, 1–12. <https://doi.org/10.1088/0964-1726/23/9/095022>.

Zhu, H. H., J. K. She, C. C. Zhang, and B. Shi. 2015. "Experimental study on pullout performance of sensing optical fibers in compacted sand." *Meas.* 73 (Sep): 284–294. <https://doi.org/10.1016/j.measurement.2015.05.027>.

Zhu, H. H., C. C. Zhang, C. S. Tang, B. Shi, and B. J. Wang. 2014. "Modeling the pullout behavior of short fiber in reinforced soil."

Geotext. Geomembr. 42 (4): 329–338. <https://doi.org/10.1016/j.geotextmem.2014.05.005>.

Zornberg, J. G. 2002. "Discrete framework for limit equilibrium analysis of fibre-reinforced soil." *Géotechnique* 52 (8): 593–604. <https://doi.org/10.1680/geot.2002.52.8.593>.